J. Am. Chem. Soc. **1993**, *115*, 1503-1507

Insertion Reactions of Monovalent Silicon: A Nonvanishing Barrier for the Silylidyne plus Hydrogen Reaction SiH + H_2

Mark S. Gordon,*,† Yaoming Xie,‡ Yukio Yamaguchi,‡ Roger S. Grev,‡ and Henry F. Schaefer III‡

Contribution from the Department of Chemistry, North Dakota State University, Fargo, North Dakota 58105, and Center for Computational Quantum Chemistry, University of Georgia, Athens, Georgia 30602. *Received July 23, 1992*

Abstract: Ab initio quantum mechanical methods have been applied to the SiH ($X\ ^2\Pi$) insertion into the H_2 molecule. The transition state has no elements of symmetry. The classical barrier height is predicted to be 5.6 ± 1 kcal/mol. The barrier is qualitatively consistent with an estimate from Jasinski's experimental reaction rates, which are much slower than those observed for the related CH + H_2, SiH + SiH_4, and SiH_2 + H_2 reactions.

Introduction

The first comprehensive study of the kinetics of monovalent silicon compound (SiR) reactions was reported by Begemann, Dreyfus, and Jasinski[1] in 1989. They examined the reactions of SiH with H_2, D_2, and SiH_4 using laser-induced fluorescence. Related experimental studies are those of Schmitt, Gressier, Krishnan, De Rosny, and Perrin[2] (SiH + SiH_4) and Nemoto, Suzuki, Nakamura, Shibuya, and Obi[3] (SiH + NO, O_2, SiH_4, and phenylsilane). These experimental investigations have been reviewed recently.[4]

The silylidyne reaction studied by Jasinski[1,4]

$$SiH(X\ ^2\Pi) + H_2 \rightarrow SiH_3 \qquad (1)$$

appears to be quite different from the valence isoelectronic carbyne reaction

$$CH(X\ ^2\Pi) + H_2 \rightarrow CH_3 \qquad (2)$$

or the analogous SiH reaction with silane

$$SiH(X\ ^2\Pi) + SiH_4 \rightarrow H_2Si\text{-}SiH_3 \qquad (3)$$

or the silylene reaction

$$SiH_2(X\ ^1A_1) + H_2 \rightarrow SiH_4 \qquad (4)$$

The CH reaction (2) with H_2 is about two orders of magnitude more rapid[5] than the SiH reaction (1). The SiH + SiH_4 reaction (3) occurs gas kinetically[1] and is also significantly faster than the prototypical reaction (1). Finally, the SiH_2 reaction (4)[6-8] has rate constants 50–100 times greater than those for reaction 1. Thus the SiH + H_2 reaction is uniformly much slower than the three related elementary reactions for which experimental data exist.

The first theoretical study of any system closely related to SiH + H_2 was that with Brooks[9] for the CH + H_2 reaction, i.e. reaction 2. Brooks showed that there is no apparent barrier for this simple insertion leading to the methyl radical. Brooks' primary result has been confirmed by higher level theoretical studies[10] and by subsequent experiments.[5] Similarly, the $SiH_2(^1A_1)$ + H_2 reaction has been shown by theory[11] and experiment[6-8] to have an activation energy no larger than 2 kcal/mol. Thus, the simplest explanation of the slowness of the SiH + H_2 reaction (1) compared to reaction 2–4 is that the latter have virtually no activation energy while the former has some activation energy. Begemann, Dreyfus, and Jasinski[1] have taken this analysis a step further by their observation that vibrationally excited SiH (v = 1) reacts with H_2 at least 3 orders of magnitude faster than SiH in its v = 0 vibrational ground state. Thus the 6 kcal/mol available to v = 1 SiH is a ballpark estimate[12] of the activation energy for reaction 1.

The purpose of the present ab initio quantum mechanical study is to locate the (presumed) transition state for reaction 1, carry out a vibrational analysis at this stationary point, and explain why there appears to be a barrier for the SiH + H_2 insertion and no barrier for the related reactions (2–4). The only previous theoretical study[13] of the SiH + H_2 potential surface was restricted to the C_{2v} least motion approach

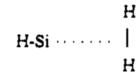

$$\text{H-Si}\cdots\cdots\begin{matrix}\text{H}\\ |\\ \text{H}\end{matrix} \qquad (5)$$

which is accompanied by a large barrier (~70 kcal/mol) due to its Woodward–Hoffmann forbiddenness. There are three imaginary vibrational frequencies associated with the least motion approach C_{2v} stationary point for SiH + H_2. Thus, the present investigation may be viewed as a search for the parts of the SiH + H_2 energy hypersurface reached by following two of the C_{2v} imaginary vibrational frequency normal coordinates.

First Theoretical Approach

The present paper is a synthesis of studies carried out independently at two different universities. The first investigation was carried out using the GAUSSIAN 88 series of programs[14] and

---

* Permanent address: Department of Chemistry, Iowa State University, Ames, Iowa 50010.

† North Dakota State University.

‡ University of Georgia.

[1] Begemann, M. H.; Dreyfus, R. W.; Jasinski, J. M. *Chem. Phys. Lett.* **1989**, *155*, 351.

[2] Schmitt, J. P. M.; Gressier, P.; Krishnan, M.; De Rosny, G.; Perrin, J. *Chem. Phys.* **1984**, *84*, 281.

[3] Nemoto, M.; Suzuki, A.; Nakamura, H.; Shibuya, K.; Obi, K. *Chem. Phys. Lett.* **1989**, *162*, 467.

[4] Jasinski, J. M.; Gates, S. M. *Acc. Chem. Res.* **1991**, *24*, 9. Jasinski, J. M. In *Frontiers in Organosilicon Chemistry*; Bassindale, A. R., Gaspar, P. P., Ed.; Royal Society of Chemistry: Cambridge, England, 1991; pp 112–121.

[5] Berman, M. R.; Lin, M. C. *J. Chem. Phys.* **1984**, *81*, 5743.

[6] Jasinski, J. M.; Chu, J. O. *J. Chem. Phys.* **1988**, *88*, 1678.

[7] Baggott, J. E.; Frey, H. M.; King, K. D.; Lightfoot, P. D.; Walsh, R.; Watts, I. M. *J. Phys. Chem.* **1988**, *92*, 4025.

[8] Moffatt, H. F.; Jensen, K. F.; Carr, R. W. *J. Phys. Chem.* **1991**, *95*, 145.

[9] Brooks, B. R.; Schaefer, H. F. *J. Chem. Phys.* **1977**, *67*, 5146.

[10] Dunning, T. H.; Harding, L. B. In *Theory of Chemical Reaction Dynamics*; Baer, M., Ed.; CRC Press: Boca Raton, Florida, 1985; Vol. 1, pp 1–69. Dunning, T. H.; Harding, L. B.; Bair, R. A.; Eades, R. A.; Shepard, R. L. *J. Phys. Chem.* **1986**, *90*, 344. Aoyagi, M.; Shepard R.; Wagner, A. F. *Int. J. Supercomput. Appl.* **1991**, *5*, 72.

[11] Gordon, M. S.; Gano, D. R.; Binkley, J. S.; Frisch, M. J. *J. Am. Chem. Soc.* **1986**, *108*, 2191.

[12] Jasinski, J. M. Personal communication, June, 1992.

[13] Duran, M.; Yamaguchi, Y.; Schaefer, H. F. *J. Phys. Chem.* **1988**, *92*, 3070.

[14] Frisch, M. J.; Head-Gordon, M.; Schlegel, H. B.; Raghavachari, K.; Binkley, J. S.; Gonzalez, C.; DeFrees, D. J.; Fox, D. J.; Whiteside, R. A.; Seeger, R.; Melius, C. F.; Baker, J.; Kahn, L. R.; Kahn, J. J. P.; Fleuder, E. M.; Topiol S.; Pople, J. A. *GAUSSIAN88*; Gaussian Inc.: Pittsburgh, PA, 1988.

0002-7863/93/1515-1503$04.00/0

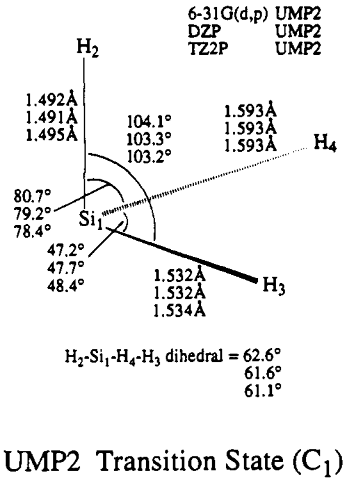

Figure 1. Transition state for the $SiH + H_2 \rightarrow SiH_3$ addition reaction. The theoretical method used was unrestricted second-order perturbation theory using three different basis sets.

the methods developed by Pople and co-workers.[15] The reactant ($SiH + H_2$), transition-state, and product (SiH_3) stationary-point geometries were initially optimized using second-order perturbation theory based on the unrestricted Hartree–Fock method (UMP2) in conjunction with the 6-31G(d,p) basis set[15] with six d-like functions on silicon with $\alpha_d(Si) = 0.395$. The transition state has no symmetry (point group C_1) and is shown in Figure 1.

For the doublet electronic states under consideration, the expectation value of S^2 should be $S(S + 1) = (^1/_2)(^3/_2) = 0.75$. At the 6-31G(d,p) UMP2 stationary-point geometries, the values of $\langle S^2 \rangle$ for the single configuration 6-31G(d,p) UHF wave functions are 0.762 (SiH), 0.833 (transition state), and 0.754 (SiH_3). Thus the molecular systems described do not result in serious methodological problems for the UHF method.

The presence of three distinct Si–H bond distances (1.492, 1.532, and 1.593 Å) at the transition state is the most interesting structural feature therein. With reference to Figure 1, the H_3–H_4 internuclear separation (1.253 Å) is much shorter than H_2–H_3 (1.999 Å) or H_2–H_4 (2.384 Å), making it clear that H_3–H_4 was formerly the H_2 entity in the $SiH + H_2$ reaction. However it is evident that this C_1 transition state does not obey Hammond's postulate,[20] which states that the transition state for an exothermic reaction (such as $SiH + H_2$) should closely resemble the reactants. With an H–H separation of 1.254 Å, there has obviously been a big change with respect to the 0.741 Å observed for isolated H_2. On the other hand, the 47.2° H_3–Si–H_4 angle makes it clear that, despite the three reasonable Si–H distance, the transition state is also removed structurally from the product SiH_3 molecule. At the 6-31G(d,p) UMP2 level of theory, SiH_3 is predicted to have C_{3v} symmetry, with an Si–H bond length of 1.467 Å and an H–Si–H bond angle of 111.1°. The latter may be compared with the experimental bond angle of 110.6°.

Given the 6-31G(d,p) UMP2 stationary-point geometries and harmonic vibrational frequencies, it is possible to use single-point energy evaluations at higher levels of theory[15] to estimate the true activation energy for reaction 1. With fourth-order perturbation theory (UMP4) and the somewhat larger 6-311G(d,p) basis set, the predicted $SiH + H_2$ activation energy is 14.1 kcal/mol. When the UMP4 results are spin projected (PUMP4),[21] the predicted activation energy is reduced to 12.3 kcal/mol. A slightly higher activation energy (12.7 kcal/mol) is predicted with the QCISD(T) method[22] using the 6-311G(d,p) basis set. The difference between the UMP4 and PUMP4 activation energies reflects the fact that there is much more spin contamination in the transition state than for the reactants. Because the QCISD(T) method does not include spin projection and there is still much room for improvement in the basis set, we estimate that the true activation energy will be significantly lower.

Second Theoretical Approach

The theoretical results just presented assume that the $SiH + H_2$ potential energy hypersurface near the transition state is qualitatively described by a single configuration. Because we know[13] that for the least motion C_{2v} pathway the reactants SiH + H_2 are described by the configuration

$$1a_1^2 2a_1^2 3a_1^2 1b_2^2 1b_1^2 4a_1^2 5a_1^2 2b_1 \qquad (6)$$

and the product SiH_3 molecule (for planar geometries) by

$$1a_1^2 2a_1^2 3a_1^2 1b_2^2 1b_1^2 4a_1^2 2b_2^2 2b_1 \qquad (7)$$

there is reason for concern about the viability of the single-configuration approximation. Therefore, in the second theoretical approach, a multiconfiguration self-consistent-field (MCSCF) method was adopted.

Specifically, the complete active space (CAS) SCF method[16,17] was used to examine the $SiH + H_2$ reaction. The MCSCF program used was that of Knowles and Werner,[18] as found in early versions of CADPAC, developed at the University of Cambridge by N. C. Handy's research group.[19] Because there are only seven valence electrons ($Si(3s^2 3p^2)$) and three hydrogen atoms) in the system under study, the full valence CASSCF is straightforward. The seven-valence-electron, seven-orbital CASSCF is designated ($7e^-$/7MO) and includes 1225 spin-adapted doublet configurations in C_1 symmetry.

Two contracted Gaussian basis sets were used in the CASSCF studies reported here. The double-ζ plus polarization (DZP) set may be technically designated

$$Si(11s7p1d/6s4p1d);\ \alpha_d(Si) = 0.5$$

$$H(4s1p/2s1p);\ \text{s functions scaled by } (1.2)^2;\ \alpha_p(H) = 0.75$$

and is due to Huzinaga, Dunning, and Hay.[23-25] The larger triple-ζ plus double-polarization (TZ2P) set is similarly labeled

$$Si(12s9p2d/6s5p2d);\ \alpha_d(Si) = 0.25,\ 1.0$$

$$H(5s2p/3s2p);\ \alpha_p(H) = 0.375,\ 1.5$$

and is due to Huzinaga, Dunning, McLean, and Chandler.[26-28]

The ($7e^-$/7MO) CASSCF stationary points were determined for the $SiH + H_2$ system via the analytic gradient CADPAC programs[18,19] using both DZP and TZ2P basis sets. For diatomic Si–H the equilibrium bond distances are 1.540 Å (DZP CASSCF) and 1.542 Å (TZ2P CASSCF), compared to experiment,[29] 1.520 Å. Similarly the H–H bond distance is 0.756 Å with both DZP and TZ2P basis sets, as opposed to experiment, 0.741 Å. The product SiH_3 molecule is predicted to be pyramidal (H–Si–H bond angles 111.1° DZP and 110.8° TZ2P) with Si–H equilibrium bond distances 1.500 (DZP CASSCF) and 1.501 Å (TZ2P CASSCF). The vibrationally averaged H–Si–H bond angle for SiH_3 is estimated to be 110.6° from ESR experiments,[30] while

---

(15) Hehre, W. J.; Radom, L.; Schleyer, P. v. R.; Pople, J. A. *Ab Initio Molecular Orbital Theory*; Wiley: New York, 1986.

(16) Roos, B. O.; Taylor, P. R.; Siegbahn, P. E. M. *Chem. Phys.* **1980**, *48*, 157.

(17) Ruedenberg, K.; Schmidt, M. W.; Gilbert, M. M.; Elbert, S. T. *Chem. Phys.* **1982**, *71*, 41.

(18) Knowles, P. J.; Werner, H. J. *Chem. Phys. Lett.* **1985**, *115*, 259. Warner, H. J.; Knowles, P. J. *J. Chem. Phys.* **1985**, *82*, 5053.

(19) Amos, R. D.; Rice, J. E. *CADPAC: Cambridge Analytic Derivatives Package, Issue 4.0*; Cambridge University: Cambridge, England, 1987.

(20) Hammond, G. S. *J. Am. Chem. Soc.* **1955**, *77*, 334.

(21) Schlegel, H. B. *J. Phys. Chem.* **1988**, *92*, 3075.

(22) Pople, J. A.; Head-Gordon, M.; Raghavachari, K. *J. Chem. Phys.* **1987**, *87*, 5968.

(23) Huzinaga, S. *J. Chem. Phys.* **1965**, *42*, 1293.

(24) Dunning, T. H. *J. Chem. Phys.* **1970**, *53*, 2823.

(25) Dunning, T. H.; Hay, P. J. In *Modern Theoretical Chemistry*; Schaefer, H. F., Ed.; Plenum: New York, 1977; Vol. 3, pp 1–27.

(26) Huzinaga, S. Approximate Atomic Functions II. Department of Chemistry Report; University of Alberta: Edmonton, Alberta, Canada, 1971.

(27) Dunning, T. H. *J. Chem. Phys.* **1971**, *55*, 716.

(28) McLean, A. D.; Chandler, G. S. *J. Chem. Phys.* **1980**, *72*, 5639.

(29) Huber, K. P.; Herzberg, G. *Constants of Diatomic Molecules*; Van Nostrand Reinhold: New York, 1979.

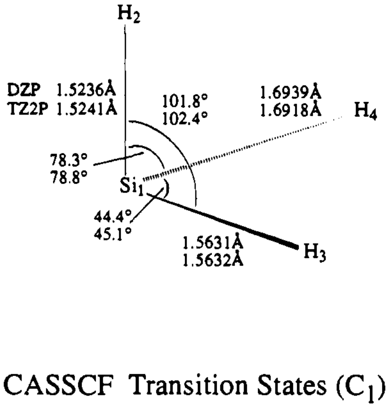

Figure 2. Transition state for the SiH + $H_2 \rightarrow SiH_3$ addition reaction. The theoretical methods used were DZP CASSCF and TZ2P CASSCF.

Table I. Zero-Point Vibrational Energies (in kcal/mol) Predicted at Several Levels of Theory for Species Involved in the SiH + $H_2 \rightarrow SiH_3$ Addition Reaction

	6-31G(d,p) UMP2[a]	DZP CASSCF	TZ2P CASSCF
SiH	3.06	2.81	2.79
H_2	6.59	6.12	6.04
reactants	9.65	8.93	8.83
transition state	11.49	9.96	9.80
SiH_3	14.03	13.14	12.94
Δ(TS − reactants)	1.84	1.03	0.97

[a] The 6-31G(d,p) basis set includes six d-like functions with $\alpha_d(\mathrm{Si}) = 0.395$.

the Si–H equilibrium bond distance is 1.477 Å at much higher levels of theory.[31] All the reactant and product geometrical predictions give bond distances that are too long, and these results confirm the well-established thesis that CASSCF wave functions introduce too much antibonding character into the wave function. This trend is expected to carry over to the predicted CASSCF transition-state geometries.

Figure 2 shows the DZP CASSCF and TZ2P CASSCF transition states for the $SiH(^2\Pi) + H_2$ addition reaction (1). The DZP CASSCF and TZ2P CASSCF transition-state structure are very similar, the largest Si–H bond distance difference being 0.002 Å. As expected, the CASSCF bond distances are larger than those predicted by the UMP2 method. The largest difference, a bit less than 0.1 Å, occurs for the $Si–H_4$ distance, which is 1.692 Å with the TZ2P CASSCF method and 1.593 Å with the TZ2P UMP2 method. The spread in the transition-state Si–H distances increases from 0.098 Å with TZ2P UMP2 to 0.168 Å with TZ2P CASSCF. In this sense the CASSCF transition state is "less symmetrical" than that predicted from the UMP2 method. However, these two very different theoretical methods yield qualitatively similar transition-state geometries. For example, the very acute H_3–Si–H_4 angle is 45.1° with TZ2P CASSCF, or 3.3° less than the analogous TZ2P UMP2 prediction.

Of greatest interest are the predicted barrier heights for the SiH + H_2 addition reaction, namely 18.0 kcal/mol (DZP CASSCF) and 18.1 kcal/mol (TZ2P CASSCF). These barrier heights may be converted to activation energies using the zero-point vibrational energies (Table I), derived from the vibrational frequencies reported in Table II. The zero-point vibrational energies are unusual in that they are larger for the transition state than for the reactants (SiH + H_2). This is because the reactant molecules have only one vibrational degree of freedom each, while the transition state has five real vibrational frequencies. The TZ2P CASSCF ZPVE's should be the most reliable and suggest that the activation energy is 0.97 kcal larger than the classical barrier height.

Of course, one purpose of the CASSCF studies was to test the reasonableness of single-configuration-based theroetical methods for the SiH + H_2 reaction. At the TZ2P CASSCF transition-state geometry, the density matrix was diagonalized and the CASSCF wave function recomputed in terms of its natural orbitals. The coefficient of the leading configuration was 0.964, corresponding to 92.9% of the wave function. Thus the SiH + H_2 system at the transition state for insertion is well described by the Hartree–Fock wave function. This finding supports the use of high-level single-reference-based methods reported in the next section. Furthermore, since nondynamical correlation effects (involving near degeneracies and rearrangements of electrons within partly filled shells) are not large for the SiH + H_2 reaction and dynamical correlation effects are not included in the CASSCF approach,[16] it is possible that the UMP2 method may provide a more reliable transition-state geometry.

Coupled Cluster Energies

Final energetic predictions were made using the single- and double-excitation coupled-cluster method (CCSD)[32] and that augmented by the perturbative treatment of connected triple excitations, i.e. CCSD(T).[33,34] Eight different predictions of the classical barrier height were made in the following manner. First, the DZP and TZ2P basis sets were used with both the CCSD and CCSD(T) methods. Second, both the UMP2 and CASSCF stationary-point geometries were independently assumed for the coupled-cluster treatments. All the coupled-cluster results are summarized in Table III.

The predicted classical barrier heights are relatively independent of the assumed stationary-point geometries. For example, using TZ2P CCSD(T) energies with the TZ2P CASSCF geometries gives a classical barrier of 9.5 kcal/mol, while the same barrier is 9.8 kcal/mol with the 6-31G(d,p) UMP2 geometries. It is of course likely that the classical barrier will be decreased with still larger basis sets and more complete descriptions of electron correlation. This theoretical prediction is consistent with Jasinski's ballpark estimate[1] (see introduction) of 6 kcal/mol.

Also noteworthy is the change in the classical barrier in going from the CCSD to the CCSD(T) method. Assuming the TZ2P CASSCF stationary-point geometries, this reduction in barrier height is 11.49 − 9.49 = 2.00 kcal/mol. With the 6-31G(d,p) geometries, the analogous difference is 11.70 − 9.76 = 1.94 kcal/mol. This finding is consistent with others[35] that suggest that connected triple excitations tend to significantly reduce theoretical barrier heights.

Because the insertion barrier for the related $SiH_2 + H_2$ reaction changes by about 4 kcal/mol at the MP4 level of theory when the basis set is increased from TZ2P (silicon) TZP (hydrogen) to MC-311++G(3df,3pd),[11] we investigated the effects of still larger basis sets on the SiH + H_2 reaction. Specifically, atomic natural orbital basis sets for hydrogen[36] (8s6p4d) → [4s2p1d] and silicon[37] (20s15p4d3f1g) → [5s4p2d1f] and [6s5p3d2f1g] are adopted. Using the UMP2/6-31G(d,p) transition-state geometry, the CCSD(T) barrier with the [5421/421] ANO basis set is 7.50 kcal/mol, and with the [65321/421] basis set, the barrier drops to 6.73 kcal/mol. Thus, increasing the basis set from TZ2P to [65321/421] decreases the insertion barrier by 3.03 kcal/mol.

The barrier lowering with larger basis sets closely parallels the reaction energy itself, which allows us to estimate remaining basis set errors for the classical barrier height. For example, changing the basis set from TZ2P to [5421/421] decreases the reaction energy by 1.67 kcal/mol (from −41.76 to −43.43 kcal/mol) and

---

(30) Jackel, G. S.; Christiansen, J. J.; Gordy, W. *J. Chem. Phys.* **1967**, *47*, 4274.

(31) Allen, W. D.; Schaefer, H. F. *Chem. Phys.* **1986**, *108*, 243.

(32) Rittby, M.; Bartlett, R. J. *J. Phys. Chem.* **1988**, *92*, 3033. Bartlett, R. J. *J. Phys. Chem.* **1989**, *93*, 1697.

(33) Raghavachari, K.; Trucks, G. W.; Pople, J. A.; Head-Gordon, M. *Chem. Phys. Lett.* **1989**, *157*, 479.

(34) Scuseria, G. E. *Chem. Phys. Lett.* **1991**, *176*, 27.

(35) Gallo, M. M.; Hamilton, T. P.; Scheafer, H. F. *J. Am. Chem. Soc.* **1990**, *112*, 8714.

(36) Almlof, J.; Taylor, P. R. *J. Chem. Phys.* **1987**, *86*, 4070.

(37) Grev, R. S.; Schaefer, H. F. Thermochemistry of C_n, SiH_n (n = 0–4), and the Cations SiH^+, SiH_2^+, and SiH_3^+: A Converged Quantum Mechanical Approach. *J. Chem. Phys.*, in press.

Table II. Harmonic Vibrational Frequencies and Infrared Intensities of SiH, H_2, SiH_3, and the Transition State for the SiH + H_2 Insertion at Three Levels of Theory

			6-31G(d,p) UMP2		DZP CASSCF		TZ2P CASSCF	
			freq (cm^{-1})	IR int (km/mol)	freq (cm^{-1})	IR int (km/mol)	freq (cm^{-1})	IR int (km/mol)
SiH	σ^+	Si–H stretching	2138	411	1969	243	1949	259
H_2	σ_g^+	H–H stretching	4610	0	4280	0	4226	0
TS	a	Si_1–H_2 stretching	2239	105	2036	89	2008	101
	a	Si_1–H_3 stretching	2044	73	1866	4	1839	3
	a	Si_1–H_4 stretching	1954	191	1401	197	1380	191
	a	H_2–Si_1–H_3 bending	1002	20	930	14	922	12
	a	H_2–Si_1–H_4 bending	802	26	734	22	706	14
	a	H_3–Si_1–H_4 bending	1866*i*		1491*i*		1587*i*	
SiH_3	e	Si–H stretching	2356	150	2177	126	2144	139
	a_1	Si–H stretching	2321	11	2147	10	2115	11
	e	H–Si–H bending	982	78	943	76	925	61
	a_1	H–Si–H bending	817	102	802	115	796	85

Table III. Total Energies (hartrees) and Relative Energies (kcal/mol) for SiH, H_2, SiH_3, and the Transition State for SiH + H_2 Insertion[d]

	SiH + H_2	transition state	SiH_3
	6-31G(d,p)[a]		
UMP2 total energies	−290.641 402 (−289.483 741, −1.157 661)	−290.617 512	−290.705 188
UMP2 relative energies	0.0	14.99	−40.03
after UMP2 ZPVE correction	0.0	16.83	−35.65
DZP CCSD single-point energies	−290.660 770 (−289.494 128, −1.166 642)	−290.641 770	
DZP CCSD relative energies	0.0	11.92	
DZP CCSD(T) single-point energies	−290.662 194 (−289.495 552, −1.166 642)	−290.645 663	
DZP CCSD(T) relative energies	0.0	10.37	
TZ2P CCSD single-point energies	−290.700 783 (−289.530 025, −1.170 758)	−290.682 138	−290.766 788
TZ2P CCSD relative energies	0.0	11.70	−41.42
TZ2P CCSD(T) single-point energies	−290.703 064 (−289.532 306, −1.170 758)	−290.687 507	−290.769 615
TZ2P CCSD(T) relative energies	0.0	9.76	−41.76
[5421/421] CCSD single-point energies	−290.721 109[b] (−289.547 877,[b] −1.173 232)	−290.705 788	
[5421/421] CCSD relative energies	0.0	9.61	−43.23[b]
[5421/421] CCSD(T) single-point energies	−290.724 414[b] (−289.551 182,[b] −1.173 232)	−290.712 469	
[5421/421] CCSD(T) relative energies	0.0	7.50	−43.43[b]
[65321/421] CCSD single-point energies	−290.723 499[b] (−289.550 267,[b] −1.173 232)	−290.709 283	
[65321/421] CCSD relative energies	0.0	8.92	−43.78[b]
[65321/421] CCSD(T) single-point energies	−290.727 064[b] (−289.553 832,[b] −1.173 232)	−290.716 335	
[65321/421] CCSD(T) relative energies		6.73	−43.98[b]
∞ relative energies		5.6[c]	−44.74[b]
	DZP		
CASSCF total energies	−290.590 952 (−289.441 352, −1.149 600)	−290.562 211	−290.655 131
CASSCF relative energies	0.0	18.04	−40.27
After CASSCF ZPVE correction	0.0	19.08	−36.07
CCSD single-point energies	−290.660 576 (−289.493 966, −1.166 610)	−290.641 393	
CCSD relative energies	0.0	12.04	
CCSD(T) single-point energies	−290.662 017 (−289.495 407, −1.166 610)	−290.645 376	
CCSD(T) relative energies	0.0	10.44	
	TZ2P		
CASSCF total energies	−290.614 969 (−289.463 508, −1.151 461)	−290.586 101	−290.677 685
CASSCF relative energies	0.0	18.11	−39.35
After CASSCF ZPVE correction	0.0	19.08	−35.24
CCSD single-point energies	−290.700 665 (−289.529 967, −1.170 688)	−290.682 346	
CCSD relative energies	0.0	11.49	
CCSD(T) single-point energies	−290.702 957 (−289.532 269, −1.170 688)	−290.687 836	
CCSD(T) relative energies	0.0	9.49	

[a] The 6-31G(d,p) basis set includes six d-like functions with $\alpha_d(Si) = 0.395$. [b] Ref 37, uses TZ2P CISD optimized geometries from ref 31. [c] Final estimate. [d] The three parts of this table used 6-31G(d,p) UMP2, DZP CASSCF, and TZ2P CASSCF stationary-point geometries, respectively.

decreases the classical barrier by 2.26 kcal/mol (9.76 versus 7.50 kcal/mol). Similarly, going from the [5421/421] basis set to the [65321/421] basis set decreases the reaction energy by another 0.55 kcal/mol (to −43.98 kcal/mol) while decreasing the classical barrier by 0.77 kcal/mol (to 6.73 kcal/mol); thus, the barrier decreases by 1.28 to 1.4 times the reaction energy. Carefully calibrated, large ANO basis set CCSD(T) studies which include core-correlation effects predict that the basis set limit reaction energy (excluding spin-orbit and other relativistic effects) is −44.74 kcal/mol,[37] or 0.78 kcal/mol in excess of that found with the [65321/421] basis set. Thus, assuming the classical barrier decreases by 1.4 times the remaining error in reaction energy, our best estimate for this barrier is 5.6 kcal/mol. At this point, it must be recognized that reoptimizing the geometry at these high levels of theory could change this value by 1 kcal/mol. Thus, our best estimate for the classical barrier height is 5.6 ± 1 kcal/mol.

Concluding Remarks

This research demonstrates that the SiH + H_2 insertion reaction has a barrier height significantly higher than those for the related CH + H_2 and SiH_2 + H_2 reactions.[9–11] Our estimate of the classical barrier for the SiH + H_2 addition reaction is 5.6 ± 1 kcal/mol.

What is the explanation for the activation energy for the SiH + H_2 addition reaction? Some understanding of the existence of a non-negligible barrier for reaction 1 may be gained by a comparison with the energetics of related reactions. For example, the reaction exothermicities for reactions 1, 2, 4, and 8, predicted by G2 theory[38]

$$CH_2(A\ ^1A_1) + H_2 \rightarrow CH_4 \qquad (8)$$

J. Am. Chem. Soc. 1993, 115, 1507-1514

are 38.4, 103.7, 53.3, and 116.5 kcal/mol, respectively. The two carbon reactions (2 and 8) are much more exothermic than their silicon counterparts, and the barriers for reactions 2 and 8 appear to be zero. The barrier height for the insertion of SiH_2 into H_2 (4) is predicted to be small (1–2 kcal/mol[11]) but nonzero, probably reflecting the greater difficulty in inserting a silicon, rather than a carbon, into the H–H bond. Because reaction 1 is 15 kcal/mol less exothermic than reaction 4, Hammond's postulate would predict a larger barrier for reaction 1. At the same level of theory, the exothermicity of reaction 3, the insertion of SiH into an Si–H bond of silane, is found to be 39.3 kcal/mol. This is essentially the same as the exothermicity predicted for reaction 1. So on purely thermodynamic grounds, one would predict similar barriers to reactions 1 and 3. The fact that reaction 1 appears to have a larger barrier very likely reflects the greater ease of insertion into an Si–H bond rather than an H–H bond. This "steric factor" has been found to play a role in the insertions of SiH_2 into a variety of X–H and X–Y bonds.[39]

The relative barrier heights for reactions 1 and 2, CH versus SiH insertion, may be viewed from an electronic point of view as well. The unpaired electron in both CH and SiH is a p orbital. Because CH_3 is essentially flat, the unpaired electron remains in a p orbital throughout the reaction. In contrast, SiH_3 is pyramidal, suggesting that the orbital containing the unpaired electron must undergo a (energy-demanding) hybridization as the reaction proceeds. The rather distorted nature of the geometry of the saddle point (Figures 1 and 2) suggests that most of this rehybridization occurs by the time the reaction reaches the transition-state region.

Acknowledgment. The research at Georgia was supported by the National Science Foundation under Grant CHE-8718469. M.S.G. was also supported by the National Science Foundation (Grant CHE-8911911) and by the U.S. Air Force Office of Scientific Research (Grant AFOSR 90-0052).

---

(38) (a) Curtiss, L. A.; Raghavachari, K.; Trucks, G. W.; Pople, J. A. *J. Chem. Soc.* **1991**, *94*, 7221. (b) Curtiss, L. A.; Raghavarachari, K.; Deutsch, P. W.; Pople, J. A. *J. Chem. Phys.* **1991**, *95*, 2433.

(39) Gano, D. R.; Gordon, M. S.; Boatz, J. A. *J. Am. Chem. Soc.* **1991**, *113*, 6711.

Thermochemistry and Ion–Molecule Reactions of Isomeric $C_3H_2^{\cdot+}$ Cations

Ming Wah Wong and Leo Radom*

Contribution from the Research School of Chemistry, Australian National University, Canberra, ACT 2601, Australia. *Received July 27, 1992*

Abstract: Ab initio molecular orbital calculations at the Gaussian-2 (G2) level of theory have been used to examine the heats of formation and ion–molecule reactions of isomeric forms of the $C_3H_2^{\bullet+}$ cation. The linear structure l–$C_3H_2^{\bullet+}$ is predicted to lie higher in energy than the cyclic form c-$C_3H_2^{\bullet+}$ by 28 kJ mol^{-1} at 0 K (or 31 kJ mol^{-1} at 298 K), energy differences significantly smaller than previous theoretical estimates (~50 kJ mol^{-1}). The calculated kinetic and thermodynamic stabilities (at 298 K) of cyclic and linear $C_3H_2^{\bullet+}$ with respect to hydrogen-atom-abstraction reactions with H_2CO, CH_3OH, CH_4, c-C_3H_6, and H_2O are consistent with experimental observations. Interestingly, the reaction of c-$C_3H_2^{\bullet+}$ with H_2O is found to be inhibited by a kinetic barrier of 23 kJ mol^{-1}. This provides a counterexample to the assumption that ion–molecule hydrogen-atom-abstraction reactions will occur (i.e., are barrier free) whenever they are exothermic except for reactions involving molecular hydrogen. Consistent with experimental observations, the reaction l-C_3H^+ + H_2 → c-$C_3H_2^{\bullet+}$ + $H^\bullet$ is calculated to be slightly endothermic (by 4 kJ mol^{-1}). The hydrogen-atom-abstraction reaction c-$C_3H_2^{\bullet+}$ + H_2 → c-$C_3H_3^+$ + $H^\bullet$ is predicted to have a small barrier (4 kJ mol^{-1}) despite a large exothermicity (91 kJ mol^{-1}). This result is consistent with kinetic studies of the reaction. Our best theoretical estimate of the heat of formation ($\Delta H_f{}^\circ{}_{298}$) of c-$C_3H_2^{\bullet+}$ is 1387 kJ mol^{-1}, agreeing well with an experimental value (1389 kJ mol^{-1}) derived from the enthalpy change for the reaction between C_3H^+ and H_2 but differing significantly from a value (1347 kJ mol^{-1}) deduced from ion–molecule bracketing reactions. For l-$C_3H_2^{\bullet+}$, our predicted $\Delta H_f{}^\circ{}_{298}$ is 1418 kJ mol^{-1}. Both the linear and cyclic isomers of $C_3H_2^{\bullet+}$ are predicted to react with CO to form strongly bound ionized ketenes; the calculated binding energies are 225 and 168 kJ mol^{-1}, respectively. The calculated structures and ionization energies of the $C_3H_2^{\bullet+}$ isomers are in good accord with recent experimental data.

Introduction

There has been considerable recent interest in the thermochemistry and ion–molecule reactions of isomeric forms of the $C_3H_2^{\bullet+}$ cation. The cyclic structure of $C_3H_2^{\bullet+}$ (c-$C_3H_2^{\bullet+}$) has been proposed[1] as a possible precursor in ion–molecule reactions which lead to the cyclic neutral molecules c-C_3H_2 and c-$C_3H^\bullet$, both of which have been observed in interstellar clouds.[2] The heats of formation and hydrogen-abstraction reactions of the $C_3H_2^{\bullet+}$ cations have been studied extensively by selected-ion flow-tube (SIFT) and flowing afterglow–SIFT (FA–SIFT) experiments.[3,4] Recent photoelectron experiments[5] have provided information on the structures and ionization energies of the $C_3H_2^{\bullet+}$ isomers.

The existence of two isomeric forms of $C_3H_2^{\bullet+}$, cyclic (**1**) and linear (**2**), was first demonstrated by Smith and Adams[3b] in 1987. They had earlier[3a] obtained two estimates of the heat of formation of one form of $C_3H_2^{\bullet+}$, 1389 and 1377 kJ mol^{-1}. This form of

---

(1) (a) Smith, D.; Adams, N. G.; Ferguson, E. E. In *Molecular Astrophysics*; Hartquist, T. W., Ed.; Cambridge University Press: Cambridge, 1990. (b) Adams, N. G.; Smith, D. *Astrophys. J.* **1987**, *317*, L25. (c) Herbst, E.; Adams, N. G.; Smith, D. *Astrophys. J.* **1983**, *269*, 329.

(2) (a) Thaddeus, P.; Vrtilek, J. M.; Gottlieb, C. A. *Astrophys. J.* **1985**, *299*, L63. (b) Matthews, H. E.; Irvine, W. M. *Astrophys. J.* **1985**, *298*, L61. (c) Vrtilek, J. M.; Gottlieb, C.; Thaddeus, P. *Astrophys. J.* **1987**, *314*, 716. (d) Yamamoto, S.; Saito, S.; Murakami, A. *Astrophys. J.* **1987**, *322*, L55.

(3) (a) Smith, D.; Adams, N. G.; Ferguson, E. E. *Int. J. Mass Spectrom. Ion Proc.* **1984**, *61*, 15. (b) Smith, D.; Adams, N. G. *Int. J. Mass Spectrom. Ion Proc.* **1987**, *76*, 307.

(4) (a) Prodnuk, S. D.; Depuy, C. H.; Bierbaum, V. M. *Int. J. Mass Spectrum. Ion Proc.* **1990**, *100*, 693. (b) Prodnuk, S. D.; Gronert, S.; Bierbaum, V. M.; Depuy, C. H. *Org. Mass Spectrom.* **1992**, *27*, 416.

(5) (a) Clauberg, H.; Chen, P. *J. Am. Chem. Soc.* **1991**, *113*, 1445. (b) Clauberg, H.; Minsek, D. W.; Chen, P. *J. Am. Chem. Soc.* **1992**, *114*, 99. (c) Clauberg, H.; Chen, P. *J. Phys. Chem.* **1992**, *96*, 5676.

0002-7863/93/1515-1507$04.00/0